RSC Advances

ROYAL SOCIETY OF CHEMISTRY

www.rsc.org/advances

Journal Name RSC Advances Dynamic Article Links ►

Cite this: DOI: 10.1039/c0xx00000x

www.rsc.org/xxxxxx

ARTICLE TYPE

Kinetic study of swelling-induced network of folds in cross-linked PS-PDMS film

Xin Xu, Xuelin Yao, Feng Chen* and Qiang Fu*

Solvent-induced mechanical instability in cross-linked poly (styrene-block-dimethylsiloxane) (PS-PDMS) film attached to a rigid substrate was systematically investigated. Through swelling with appropriate solvent vapor, a unique network of folds could be constructed successfully without the wrinkle-to-fold transition. Instead, small holes resulted from mesostructural organization of PS-PDMS form as nuclei to induce formation and growth of invaginated folds resembling crease and then constructed the network of invaginated folds. The complete network of sharp folds could be obtained after the two edges of valley were combined into sharp fold. The morphology and kinetics were closely relative to solvent solubility parameter and saturated vapor pressure. We varied the ratio between a relatively good solvent vapor and a poor solvent vapor, and so produced a slower dynamic process to precisely control the surface morphology. Poorly ordered cylinders with varied sizes resulted from strong cross-linking and spatial restriction imposed by network of folds could be obtained.

1. Introduction

A constrained thin film on a rigid substrate can lead to the spontaneous formation of various kinds of ordered structures under adequate compressive stress.[1-8] This phenomenon is commonly acknowledged as mechanical instability, including wrinkling,[9-12] folding,[13-15] and creasing.[16, 17] In general, periodic sinusoidal wrinkle can be constructed by compressing a crust bonded to a soft layer. In this case, after further increasing compressive stress, localized fold will be produced via a wrinkle-to-fold transition. In principle, however, crease structure results from the compression of a soft layer attached to a rigid foundation. Despite different formation condition, constructing a two-layer structure whose neither modulus nor chemistry is matched prior to loading stimuli is the most fundamental procedure to develop intricate surface patterns. In most case, in order to form the two-layer structure, various cross-linking technologies often be carried out, including chemical cross-linking,[18] UV-ozone cross-linking,[19] and plasma induced cross-linking.[20] In fact, the difference of molecule modulus between top layer and lower layer closely related to cross-linking intensity can greatly influence the final pattern morphologies and kinetics. Furthermore, varying external stress will prompt the emergence of diverse surface morphologies with different characteristic dimensions. More recently, mechanical instability has played a significant role in many applications, including sensors,[21] micro-fluidic devices,[22] microlens arrays,[23] responsive coatings,[24] and microfabrication.[25, 26]

Unconstrained film can expand three-dimensionally and isotropically without releasing interior compressive stress during solvent swelling. When comes to polymer thin film attached to a rigid substrate, however, the deformation in lateral dimension is so small that the expansion only occurs in direction normal to the substrate giving rise to an equi-biaxial compressive stress.[27] Subsequently, the in-plane compressing pressure increases gradually with swelling time, which leads to an increase of mechanical instability.[18, 28] Eventually, a drastic surface undulation will result in nonhomogeneous surface deformation. Once swelling degree is beyond a threshold value, compressive stress can be relieved locally to generate a variety of periodic surface patterns. For instance, Hayward *et al*. have demonstrated this critical linear deformation of poly (acrylamide-*co*-sodium acrylate) hydrogel generating creasing instability is about 1.5 and almost independent of gel thickness and modulus.[18] When the film is weakly bounded to rigid substrate, the serious swelling even can induce delamination or large-scale folds with a characteristic dimension nearly equal to the film thickness.[29, 30] To precisely control pattern morphologies and obtain excellent surface properties, the dynamics of mechanical instability induced by solvent permeation should be understood more clearly.

In recent years, much works have focused on study of swelling-induced mechanical instability in homopolymer or random copolymer films,[31, 32] but few studies on the dynamics of fold structure of ultra-thin cross-linked block copolymer (BCP) film swelled by solvent vapor, to our best knowledge, have been reported. Under solvent annealing, the rearrangement of BCP molecules, known as self-assembly, can lead to various ordered nanostructures with nanoscale dimensions.[33-35] Therefore, if BCP film is slightly cross-linked, the cross-linked polymer network is too small to restrict the molecular movement. Thus, surface molecules will be rearranged because of the mismatch between the integer multiple of the characteristic spacing and initial film thickness to form holes or islands finally.[36-38] Nevertheless, too high cross-linking degree will inevitably prevent BCP self-assembly or even freeze the movement of chain segments. In this case, swelling-induced stretch of chains will be restricted by

elastic recovery of highly cross-linked network. [39] That is, the swelling degree is not forever proportional to swelling time but reaches a saturated value dependent of cross-linking degree.[40] Once the osmotic pressure is larger than the critical value, BCP film surface will be forced to buckle into ordered surface patterns. Therefore, surface instability of cross-linked BCP films is worth to research profoundly.

Here, we systematically presented a dynamic study of cross-linked PS-PDMS film confined on a rigid substrate through combining the swelling-induced mechanical instability and self-assembly of PS-PDMS. We employ hyperthermal hydrogen induced cross-linking (HHIC) as a cross-linking approach to construct a two-layer structure, then to further investigate the unique mechanism of swelled PS-PDMS film. Our results suggested this network of folds is closely relative to rearrangement of PS-PDMS molecules during annealing. More significantly, the solvent-induced hole structures could induce the growth of invaginated folds with a valley, and then evolved into sharp folds. Finally, the network of sharp folds formed with a characteristic amplitude dependent of swelling time. By investigating further the impact of solvent solubility parameter and saturated vapor pressure on network of folds, we clearly understood the essential conditions of forming network of folds. However, after etching PS-PDMS film, few long-range cylinders could be gained and many cylinders with random alignment isotropically distributed in network of folds. This suggests that it is a challenge that can not be overcome until a moderate cross-linking is imposed to greatly improve well-ordered rearrangement of self-assembly for cross-linked PS-PDMS film.

2. Experimental section

2.1. Materials

The asymmetric block polymer of PS-PDMS exhibiting cylinders in bulk with overall molecular weight of 42 Kg/mol (Mn, PS=31 Kg/mol, Mn, PDMS=11 Kg/mol, Mw/Mn=1.10) and with PDMS volume fraction of 27.8% and polystyrene (PS) (Mn=25 kg/mol, Mw/Mn=1.04) were purchased from Polymer Source, Inc.; Polydimethylsiloxane (PDMS) (Sylgard 184) was purchased from Dow Corning. 1, 2-dichloroethane, tetrahydrofuran (THF), toluene, chloroform, acetone, n-hexane, ethanol used as received were obtained from Aldrich.

2.2. Sample preparation

PS-PDMS was homogeneously dissolved in 1, 2-dichloroethane solvent for a certain time to generate 0.5 wt% polymer solution. Moreover, PS was homogeneously dissolved in 1, 2-dichloroethane solvent to create 0.5 wt% polymer solution, while PDMS without adding cross-linker was homogeneously dissolved in toluene solvent to produce 0.5 wt% polymer solution because toluene instead of 1, 2-dichloroethane is a good solvent for PDMS. Subsequently, the 0.5 wt% solution was spun coated onto mica wafer at speed 3000 rpm for 30 s, the thickness is about 45 nm same as previous works.[41] Initially, the films were treated by HHIC for 30 s to create a two-layer structure. The hydrogen plasma was maintained with 30 w of operating power. And then, a dose of solvents were placed in a closed vacuum desiccator. Eventually, the cross-linked films were placed on the perforated platform above the solvent to be swelled under saturated vapor pressure at room temperature. After swelled for selected time, the films were got out immediately by removing saturated vapor. The mixture of THF and ethanol solvents was generated by varying the volume ratio of two components. To gain the self-assembled patterns, the PS-PDMS films after solvent vapor treatment were first treated with a CF_4 (10 sccm) plasma for 10 s followed by an O_2 (10 sccm) plasma for 20 s with a reactive ion etching (RIE) powers of 50 and 90 W, respectively. In this etching, PS component disappeared while the PDMS component was oxidized to form silica on the substrate. The etching process was accomplished in Minilock-Phantom III (Trion Technology, Inc., US).

2.3. Characterization

The surface morphology of the film was investigated by atomic force microscopy (AFM) operating in a tapping mode using an instrument with a SPI4000 Probe Station controller (SIINT Instruments Co., Japan) at room temperature. The height contrast images were collected. Olympus tapping mode cantilevers with the spring constants ranging from 51.2 N/m to 87.8 N/m (as specified by the manufacturer) were used with a scan rate in the range of 0.8-1.2 Hz.

3. Results and discussion

3.1. The network of folds of cross-linked PS-PDMS film during vapor swelling

The ultra-thin two-layer films attached to mica substrate were successfully constructed by cross-linking PS-PDMS films using HHIC technique with an adequate power. Both PS and PDMS chains where selective cleavage of C–H bonds is produced in the presence of hydrogen plasma can be cross-linked.[42-45] The typical surface morphologies are characterized by AFM. Fig. 1a shows the AFM height image of pure PS-PDMS film. The surface is very flat without typical surface undulation, but some small holes

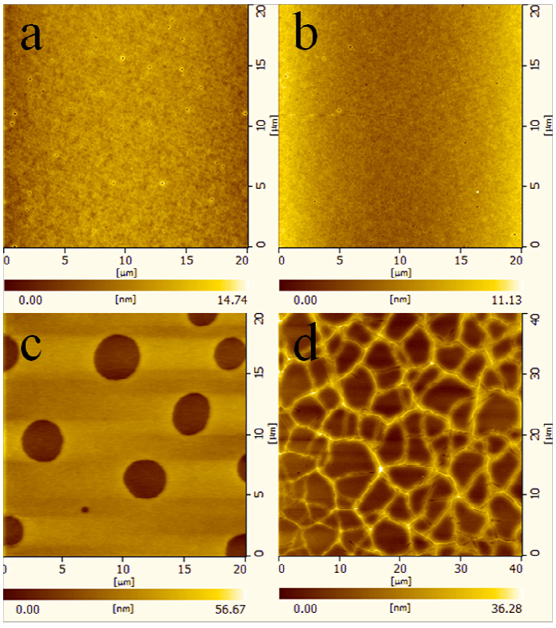

Fig. 1 AFM height images of surface morphologies produced from (a) pure PS-PDMS and (b) cross-linked PS-PDMS before swelling. The surface morphologies of (c) pure PS-PDMS and (d)

cross-linked PS-PDMS swelled for 6 h in THF vapor.

can be obviously observed. For the spin-coated BCP film, the formation of these holes which are internal defects resulting from molecular organization during solvent volatilization is a common phenomenon. Small holes have not disappeared and are reserved completely for the cross-linked film (Fig. 1b). In addition, in consequence of a short application time of HHIC, the coarsening into larger holes does not occur. Without regard to these defects, the surface is also very smooth simultaneously. Therefore, it is explicit that the intensity of HHIC is small enough not to etch film surface. In a word, this HHIC condition ensures the completeness and flatness of PS-PDMS films to further study.

AFM observation confirms that the bigger holes with 25±2 nm depth emerge for the pure PS-PDMS film during THF swelling for 6 h (Fig. 1c). This is because that the mismatch between the minimum in Gibbs free energy and the initial free energy impels realignment of PS-PDMS molecules. To satisfy the minimum in free energy, the film thickness need to be equal to the integral multiple of diameter of cylinders or else islands and holes will form directly. In the presence of cross-linking, however, a complete network of sharp folds with irregular polygonal domains can be observed obviously. Besides, no holes and islands analogue to the result of pure PS-PDMS film after annealing emerge distinctly, which reveals that the cross-linked films may have not reached equilibrium or the equilibrium mechanism is not same to that of pure films during solvent swelling. However, Fig. S1a and S1b (seen form supporting information) show that the PS and PDMS films cross-linked with the same condition are swelled for 6 h upon exposure to the THF vapor respectively, but no mechanical instability is generated. This result is not same as that of Kramer *et al*.[46] In their experiment, the swelled silica/dPS-P2VP film generated wrinkling instability. Meanwhile, the swelled silica/P2VP film produced creasing instability. They speculated that the instability in silica/dPS-P2VP did not arise necessarily from mesostructural organization of BCP. However, our result indicates that the network of folds is closely relative to mesostructural organization for swelled PS-PDMS film while can not be produced for PS and PDMS film.

3.2. Nucleation and growth of the network of folds

The cross-linked PS-PDMS films placed in THF solvent vapor were treated with different swelling time at room temperature. Fig. 2 gives the evolution of the surface morphology of cross-linked PS-PDMS films. For short swelling time equal to 2 h, the irregular holes exist at initial stage of continuous swelling (Fig. 2a). Though releasing compressive stress slightly deforms these holes, apparently coarsening is produced for most of hole structures when compared with the circular holes without exposure to THF vapor (Fig. 1b). Through carefully observing the hole structure (Fig. 2e), the raised hole rim inhibit the tendency to grow bigger, which leads to a preferential accumulation of compressive stress increasing the local mechanical instability.[47] In this case, the swelling degree does not reach the threshold value, thus generating an in-plane compressive stress which does not exceed that arising from the elastic recovery of cross-linked polymer network. Upon further swelling for 3 h, in some areas of the film, a few invaginated folds with a valley resembling crease appear and small holes do not disappear immediately (Fig. 2b). By observing the corresponding enlargement (Fig. 2g), some holes start to deform seriously to form a short tail-like structure. In this case, the linear swelling degree is beyond the critical value. Indeed, it is a challenge to accurately measure the swelling degree for ultrathin film (~45 nm). The invaginated structures gradually form along the radical direction of circular holes. Meanwhile, these results manifest indirectly the compressive stress focuses on the peripheral direction. It has been demonstrated that the direction releasing stress is normal to the direction generating stress by much works.[48, 49] In fact, the depth of hole (pointed out by red arrow in Fig. 2f) is ~23 nm while that of middle part of left invaginated fold is ~10.5 nm. In Fig. 2i, the two edges of the valley in the invaginated fold produce a slight out-of-plane bulge (~3 nm). This result demonstrates the structure is essentially invaginated fold and not the crack pattern. In general, desiccation, rather than swelling, results in crack patterns whose depth can approximate the film thickness. Particularly, the crack will sustain even when the swelling is prolonged. Instead, the sharp folds will be constructed after a long time of swelling in our results (Fig. 3a). In summary, the average depth of invaginated fold is lower than that of hole center and the hole with the fold is apparently smaller than that without fold simultaneously. Hence, it is concluded that the invaginated fold grows from the hole rim and extends outward radical direction of hole.

Remarkably, when the film is swelled for 4 h, the Y-shaped folds with invaginated valley are constructed gradually (Fig. 2c). A lot of long striped folds whose lengths are far more than film thickness grow from the junction points. In this case, Y-shaped folds including three stripes are commonly observed and only a few single striped folds are present. However, no a complete network forms and these folds spread independently without touch. The invaginated fold does not propagate straightly from the junction point due to the mutual interference with each other. To study Y-shaped folds in more detail, coexistence of a Y-shaped fold and a single striped fold can be seen (Fig. 2g). It is clearly observed the junction point is actually the previous mentioned hole. Indeed, the irregular intersection angle between the two folds, for the Y-shaped structure, is close to 120 °. A correspondingly gradual decrease from hole (~16 nm) to the end of fold (~3 nm) is observed. After swelled for 5 h, the film surface fabricates a complete network of invaginated folds (Fig. 5d). Initially, the Y-shaped folds continue to grow, subsequently each ends of them start to collide, and then a few folds connect together when the two ends of two folds directly bond while most of fold growths are prevented by mutual interference. Finally, the network texture of invaginated folds with varied characteristic distance emerges immediately. There is no obvious hole in the center of Y-shaped fold with ~5 nm depth which is smaller than the depth of the previous holes (Fig. 2h). The hole progressively grows smaller to coalesce into a junction point under the condition the folds progressively grow longer. The network structure extremely limits the lateral growth of folds, thus the average stripe depth is uniform and about 5 nm same to that of center. Significantly, the few observed holes are not the previous holes but the newly formed features resulted from asynchronous rearrangement of PS-PDMS molecules.

The typical transition from invaginated folds to sharp folds and

the complete network of sharp folds with different spaces are observed (Fig. 3a) when the film is swelled for 6 h. The distinctly observed coexistence of invaginated folds and sharp folds and inhomogenous network of folds demonstrate the stable network has been formed incompletely. Significantly, a part of

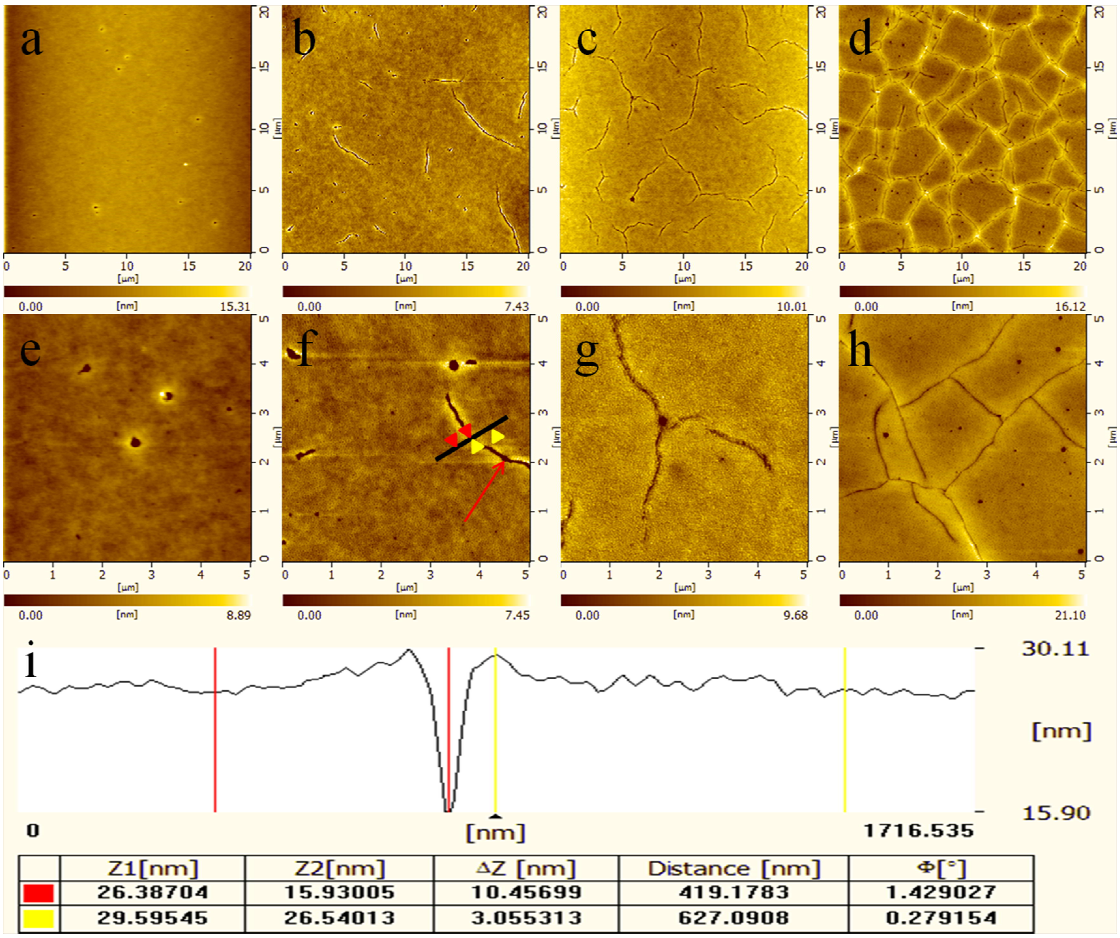

	Z1[nm]	Z2[nm]	ΔZ [nm]	Distance [nm]	Φ[°]
	26.38704	15.93005	10.45699	419.1783	1.429027
	29.59545	26.54013	3.055313	627.0908	0.279154

Fig. 2 (a-d) AFM height images and (e-h) corresponding enlargement images of cross-linked PS-PDMS films after swelled in saturated THF vapor for (a, e) 2 h, (b, f) 3 h, (c, g) 4 h, and (d, h) 5 h respectively. (i) The corresponding cross-sectional profile along the black line in (f).

invaginated folds have not transformed to sharp folds, suggesting that the newly generated holes will induce more invaginated folds when swelling time is prolonged. In addition, the strong effect of squeezing in junction point results in the fact that the junction point of folds is higher than surroundings since folds confront strong resistance in this point to terminate fold growth. By closely inspecting the area near sharp folds, a gentle height gradient is found from the fold to the network center, as shown in the cross-sectional image (Fig. 3e). This illustrates that there is a surface migration that the PS-PDMS molecules in the network center are accumulated in the area around fold. A sharp fold similar to sinusoidal pattern is found since no valley is in the peak. The edges of invaginated fold grow vertically and laterally simultaneously, which generates delamination resulting in combination of two edges and resulting disappearance of valley. As a result, the relatively complete and stable network of sharp folds is successfully constructed after 6 h swelling. In fact, Stone *et al*. have demonstrated the network of folds can be constructed through nucleation, growth, and intersection for cross-linked polyurethane film.[50] They have denoted nucleation can appear in the local area without induction of other structures and a wrinkle-to-fold transition is necessary to generate well-identified closed domains. However, in our study, we can clearly observe that the small hole resulted from mesostructural organization as nucleus can induce invaginated fold growth, transform to sharp fold, and then fabricate a network of sharp folds finally. However, no wrinkled state is observed to construct the network of folds. Therefore, the mechanisms of nucleation and growth are different so that the evolution of network of folds in our system is worthwhile to study. In contrast, such slow kinetics induced by vapor swelling contributes to clearly understand each developmental process.

In fact, the network of folds is extremely stable once it has been formed even though the film is subjected to long-time swelling. A series of images of network of folds are shown in Fig. 3b-d by prolonging the swelling time. Obviously, a tendency toward the denser network is present. As swelling time increases, more invaginated folds develop and transform into sharp folds.

Fig. 4 gives the evolution of the average amplitude (A) of network of sharp folds (measured in the middle of the fold) with

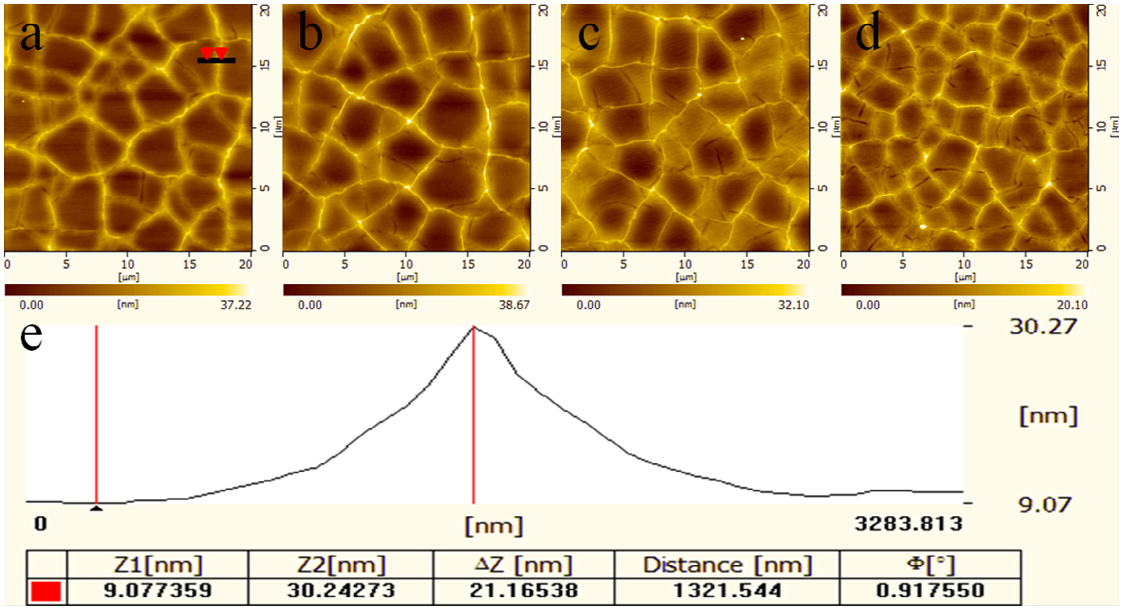

Fig. 3 AFM height images of cross-linked PS-PDMS films after swelled in saturated THF vapor for (a) 6 h, (b) 12 h, (c) 18 h, and (d) 24 h. (e) The corresponding cross-sectional profile along the black line in (a).

the swelling time. The relationship can be divided mainly into two stages. In the first stage, the average amplitude increases with increasing swelling time. For the film swelled for 6 h, A=22.05 nm, and increased to A=27.22 nm for the film undergoing 12 h of swelling. The increase of average amplitude reflects that increasing compressive stress can strongly attribute to the surface migration, and then result in an increasing accumulation in the folds and the formation of a more complete network. In second stage, however, further prolonging swelling time gives rise to a decrease of average amplitude. When the film is swelled for 18 h,

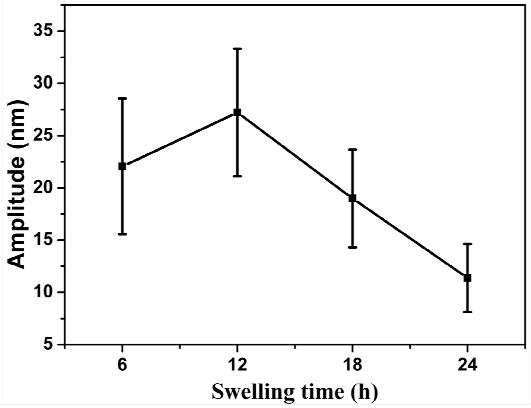

Fig. 4 The amplitude of sharp fold of cross-linked PS-PDMS film treated by THF saturated vapor as a function of swelling time.

the average amplitude decreases to A=18.99 nm. A sequential decrease to A=11.38 nm can occurred after swelling the film for 24 h. This decrease is the result that the sufficiently complete and stable network of folds resists the migration from network center to terminate vertical growth. Whereas the constrained migration produces the gradually uniform surface in whole network and constructs more sharp folds. Even though deviation of amplitude (~6 nm) is so considerable, it has a little influence on the evolution of the vertical growth of sharp fold. In addition, the significant deviation reflects the asynchronism of vertical growth and migration behavior. Note that, the gradually slower growth rate of the complete and stable network of folds with swelling time is closely relative to the saturated swelling degree. Once the swelling degree reaches this value, unceasingly increasing swelling time will not change the swelling degree. Accordingly, in our results, we can conclude that long duration of swelling has a little influence on the development of the network structures, but maintaining this saturated swelling degree is conducive to self-regulation of network of folds.

3.3. Effect of solvent vapor on network of folds

As discussed above, the morphologies of cross-linked PS-PDMS films are strongly dependent on swelling degree closely related to solvent property. For cross-linked PS-PDMS films in contact with saturated THF vapor, the relatively stable and complete network of folds has been formed after the film is swelled for 6 h. In general, the folds can form and develop under the effect of solvent while be reserved when the film is dry without osmotic pressure.[30, 31] More specifically, in our results, the formation of fold needs to be swelled for at least 3 h, but the velocity that the film becomes dry is so fast (about a few seconds) because of rapid vaporization of low boiling point solvent that the surface structure can be reserved completely. To reveal the influence of solvent vapor on the morphologies of PS-PDMS ultra-thin film, a series of low boiling point solvents were used. The corresponding solubility parameters and saturated vapor pressures are listed in Table 1. In bulk, the solubility parameters of PS and PDMS chains are 9.1 and 7.4 $cal^{1/2}cm^{-3/2}$, respectively. The spin-coated PS-PDMS films with same thickness were swelled for 6 h upon exposure to different saturated solvent vapor, and the AFM height images are shown in Fig. 5a-c. Only toluene and chloroform vapor (the strongly interactional solvents for the PS) can give rise

to fold formation (Fig. 5a and b), although the incomplete network of invaginated folds with valleys is present during treatment with saturated toluene vapour (Fig. 5a and f). The significant difference of kinetic process in THF vapor and that in toluene vapor is mainly the result of difference between two saturated vapor pressures. The saturated vapor pressure of toluene is much less than that of THF, thus the less solvent adsorption leads to smaller in-plane compressive stress. By contrast, the complete network of folds has been constructed when the film is swelled in chloroform vapor (Fig. 5b and g). The enough high saturated vapor pressure mainly affects the resulting morphologies despite the small difference between two solubility parameters.

Table 1. Solubility parameters and corresponding saturated vapor pressures of solvents at 298 K

Solvents	δ (cal1/2cm-3/2)	p * (kPa)
Tetrahydrofuran	9.5	23.46
Toluene	8.9	3.89
Chloroform	9.3	30.71
Acetone	9.8	30.60
n-hexane	7.3	20.12
Ethanol	12.9	7.81

δ: solubility parameter[51] and p *: saturated vapor pressure.

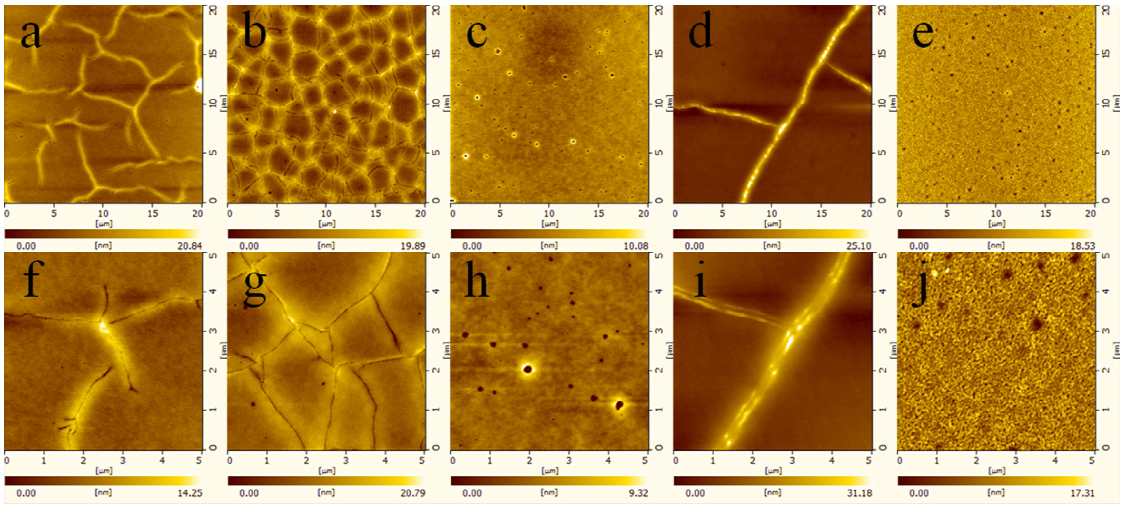

Fig. 5 (a-e) AFM height images and (f-j) corresponding enlargement images of cross-linked PS-PDMS films after swelled for 6 h in saturated vapor of (a, f) toluene, (b, g) chloroform, and (c, h) acetone; and after swelled for 24 h in (d, i) acetone vapor, and (e, j) n-hexane, respectively.

However, randomly distributed small holes can be created by using acetone vapor (a weakly interactional solvent for the PS) as the swelling agent (Fig. 5c) for a 6 h swelling treatment. By closely inspecting the enlargement (Fig. 5h), some holes have a slight deformation. By comparison to the morphology of the original cross-linked film (Fig. 1b), the amounts of holes greatly increase and the sizes of them also become bigger apparently. Obviously, some rims of bigger holes which bulge outward tend to create invaginated folds. This predicts that it is currently at the initial stage of fold formation and the film is subject to an inappropriate swelling degree below the critical value. In fact, prolonging the swelling time can give rise to emergence of the network of folds (Fig. 5d). In the condition of a 24 h swelling treatment with saturated acetone vapor, the network is more tremendous and sparser (Fig. 5i). In this case, the two edges of invaginated fold do not coalesce into a sharp fold. This demonstrates that solubility parameter is more sensitive to network formation even though the saturated vapor pressure is enough high. Remarkably, the great kinetic difference just is resulted from the tiny difference between two solubility parameters.

The morphology of cross-linked PS-PDMS film exposed to the selective solvent vapor for the PDMS is also measured. Fig. 5e shows the AFM height image of the film swelled in saturated n-hexane vapor (a strongly interactional solvent for the PDMS). Note that, no fold forms but a few small holes without deformation can be produced accompanying with strong surface fluctuation even if swelling time is prolonged to 24 h. Even though the used PS-PDMS is a PS-rich block polymer, the network of folds is induced by the mesostructural organization which is independent of whether the BCP is PS-rich or PDMS-rich. Therefore, this directly indicates that swelling PS chains is a more effective approach than swelling PDMS chains to fabricate network of folds. By carefully observing the enlargement (Fig. 5j), the intense sinusoidal wrinkles over the whole surface are generated. Indeed, it is reasonable that no fold forms in the solvent vapor (a very weakly interactional solvent for each chain). For instance, by using ethanol vapor to swell the PS-PDMS film for 24 h, only a few small holes with the constant size can be observed (Fig. S2). In summary, the solvent solubility parameter and saturated vapor pressure play key roles in surface morphologies. Only when the solubility parameter is close to that of PS will the network of folds be constructed. When the solubility parameter is more deviated from 9.1 or the saturated vapor pressure is too small, it is harder to construct the complete network. Hence, it is reasonable that the influence of solubility parameter and saturated vapor pressure on the surface morphologies can be exploited to precisely control the final structures during solvent swelling.

3.4. Morphology of cross-linked PS-PDMS film during mixed

solvent vapor swelling

Previous work has demonstrated ethanol vapor is useless to construct network of folds while using THF vapor is an effective approach to form network. The relatively complete network of folds has been created by using THF saturated vapor as swelling agent after 6 h of treatment. As discussed above, saturated vapor pressure strongly affects the growth rate of the network. Therefore, using the mixed solvent vapors generated by mixing THF and ethanol solvents (a two-miscible-solvent system) can slow down the kinetic rate to clearly enrich the understanding of the formation of network of folds and the unique nucleation. Fig. 6a-d show the morphologies of cross-linked PS-PDMS films swelled by the mixed vapors evaporated from the mixed solvents with THF/ethanol volume ratio of 8:2. A few small circular holes can be observed when the film is swelled for 3 h (Fig. 6a). By contrast, more small holes are generated but the size of holes has not been bigger (Fig. 6b) after the film is swelled for 4 h. In fact, the formation of invaginated folds can be seen after swelling the film for 5 h (Fig. 6c). Meantime, some folds have contacted with each other but not formed a complete network. After the film undergoes a 6 h swelling treatment, a complete network of folds has been generated (Fig. 6d). It is obvious that the fold peak is a valley which has not coalesced. By comparison, the valley has coalesced into a sharp fold during THF swelling. In the case that the partial pressure of saturated THF vapor is smaller than pure saturated THF vapor pressure, swelling films by the mixed solvent vapor decreases the growth rate. The slower dynamic process is beneficial to control morphology evolution.

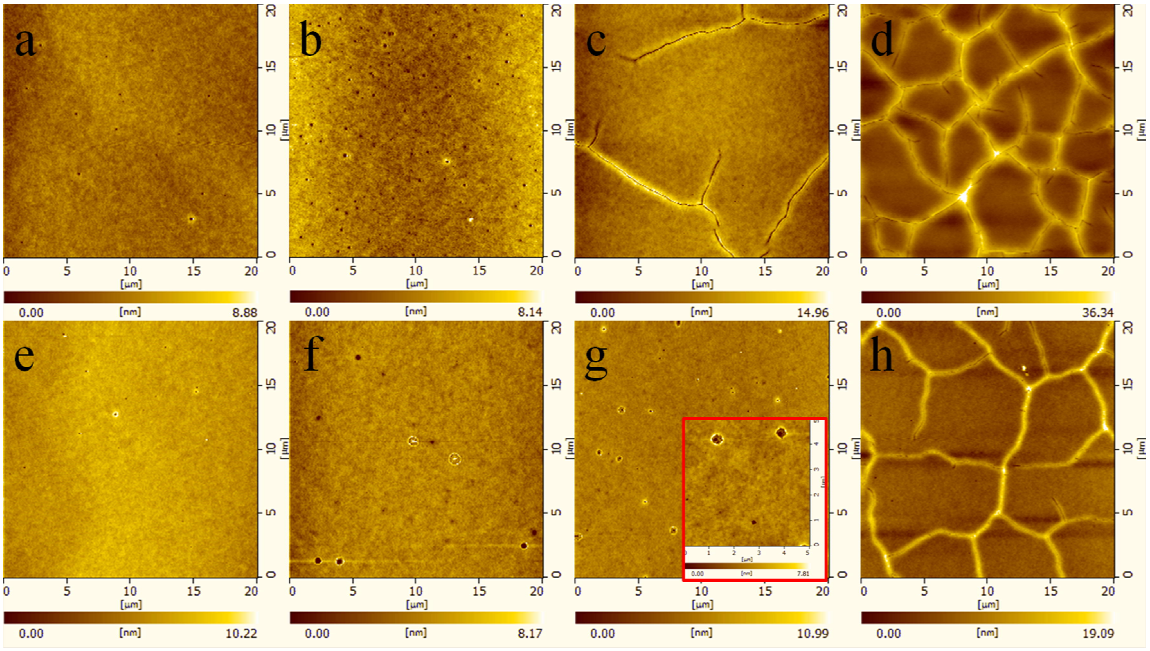

Fig. 6 AFM height images of cross-linked PS-PDMS films after swelling in mixed vapors evaporated from mixed solvents with THF/ethanol volume ratio of (a-d) 8:2 and (e-h) 6:4 for (a, e) 3 h, (b, f) 4 h, (c, g) 5 h, and (d, h) 6 h, respectively.

Further decreasing the saturated vapor pressure of effective solvent by changing the volume ratio of two solvents to 6:4 can lead to a slower kinetics. Fig. 6e-h show a series of AFM height images of cross-linked PS-PDMS films in these mixed solvent vapors. Only fewer small holes can be observed after swelling the film for 3 h (Fig. 6e), as compared to Fig. 6a. Prolonging swelling time to 4 h (Fig. 6f) generates the coexistence of more small holes and some annular ridges. In addition, the annular ridge with fluctuant roughness is possibly resulted from impurity. As shown in Fig. 6g, the greater swelling degree induces the presence of more and bigger holes for the film swelled for 5 h. From the corresponding enlargement, a few smaller holes are in interior of small holes and elastic instability is generated in the hole rim with waved deformation owing to serious stress accumulation. Indeed, after the film is swelled for 6 h, the network of folds with low amplitude is observed in Fig. 6h. During this mixed vapor swelling, the lower partial vapor pressure postpones development of hole structures. Therefore, we clearly understand that the small holes undergo the trend toward bigger and more before they initiate deformation. Most importantly, the small hole rim undergoing an accumulation of compressive stress gives rise to a gradually increased fluctuation before inducing the invaginated fold. However, lower saturated vapor pressure readily induces appearance of more intricate and irregular structures.

3.5. Self-assembly of cross-linked PS-PDMS films

We further studied self-assembly behavior of cross-linked PS-PDMS films and so RIE was carried out to etch film surface to reveal the ordered nanostructures. In fact, the coexistence between monolayer and bilayer of cylinders aligned parallel to substrate can be attained after the pure PS-PDMS film is swelled in THF vapor for 6 h (Fig. S3). The average domain spacing determined from the AFM image is about 30 nm. In addition, the nanopatterns actually are the silica residues since the PS block is removed entirely and the PDMS block is converted into silica during etching process. As mentioned above, a migration of PS-PDMS molecules leads to accumulation in fold. Fig. 7 shows a series of typical AFM height morphologies of cross-linked thin film of PS-PDMS swelled in THF vapor for 6 h after etching. As

shown in Fig. 7a, the morphology of network of folds is retained completely though the film is subjected to etching process. The valley in fold peak is obviously present after etching. Only cylinders perpendicular to substrate with varied sizes are produced in the areas around folds. Remarkably, some spherical

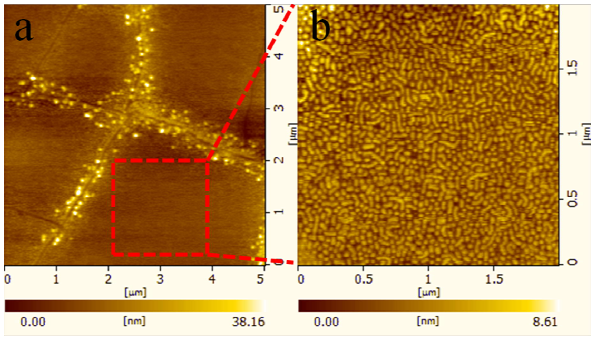

Fig. 7 Series of AFM height images of cross-linked PS-PDMS films during THF swelling for (a, b) 6 h after RIE etching. (b) zoom-in height image of the square box in (a).

silicas with about 100 nm are found in the folds, which suggests that the confined space with steep height gradient imposes restrictions on hexagonal arrangement of cylinders perpendicular to substrate. Accordingly, the cylinders in fold arrange compactly so as to fabricate bigger and denser nanostructures. Fig. 7b shows the zoom-in height image of the square box in Fig. 7a. No nanopatterns with long-range order analogous to the result of Fig. S3 can be observed in interior of network of folds, while a variety of short cylinders and spheres distribute randomly. We can speculate that the observed spheres are essentially cylinders perpendicular to substrate and some short cylinders are probably cylinders parallel or oblique to substrate. These fairly disordered cylindrical nanostructures reveal that the morphology of cross-linked film under saturated THF vapor swelling is far away from equilibrium. Therefore, the self-assembly is restricted effectively but can still be carried out. In comparison to the result of pure sample, the domain spacing does not change. However, both network of folds and cross-linked polymer networks will have a great influence on self-assembled nanostructures.

3.6. Schematic representation of evolution of formation and development of network of folds for cross-linked PS-PDMS film

The introduction of solvent-induced compressive in-plane stress into cross-linked PS-PDMS film will give rise to the construction of a unique network of folds. In our study, during appropriate vapor swelling, the evolution of formation and development of network of folds is hypothetically described as shown in Fig. 8 (seen from the angle perpendicular to the surface). At first, without swelling, the cross-linked film surface maintains flatness and integrity. When solvent vapor is absorbed into film, cross-linking can naturally constrain molecular movement theoretically. However, the mismatch between initial film thickness and the integer multiple of the characteristic diameter for cylinder forming system will impel formation of terrace structure. Hence, the balance between two opposite effects will lead to form a series of small holes with different sizes forming preferentially at internal defects (Fig. 8a). To satisfy this changeable balance resulted from increasing swelling degree, the small holes will become more and bigger with swelling time and then increase to a saturated value (Fig. 8b). Significantly, for a complete film, the small holes as defects undergo a preferential solvent absorption to generate an accumulation of compressive stress. Once the swelling time is long enough, the hole rim starts to fluctuate and deform (Fig. 8c). The invaginated fold will be created from outer edge of the hole in direction normal to peripheral direction to release the local stress. In other words, the small holes actually are nuclei to create invaginated fold and subsequent sharp fold.

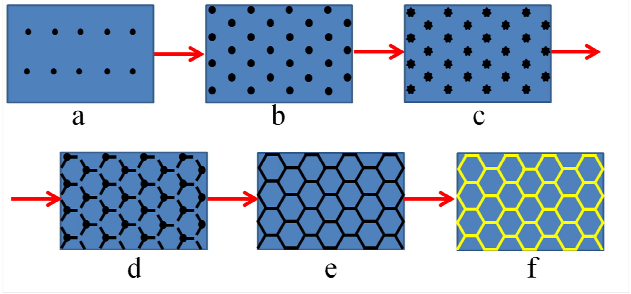

Fig. 8 Schematic diagram depicting the evolution of constructing network of folds on the surface of cross-linked PS-PDMS film during adequate solvent vapor swelling: (a). solvent vapor swells the film and molecular rearrangement induces small holes; (b). more and denser small holes form when the swelling time is prolonged; (c). accumulation of compressive stress in hole rim leads to deform and fluctuate; (d). small holes induce formation complete network of invaginated folds is constructed; (f). the transition from invaginated fold to sharp fold induces complete network of sharp folds. The black represents dent and the yellow represents bulge.

As the swelling time is prolonged, The Y-shaped fold with invaginated valley growing laterally and in three different directions is the most stable morphology to construct network of invaginated folds (Fig. 8d). At this time, the small holes gradually vanish in a junction point. Simultaneously, the invaginated folds grow to contact with each other and the depth of them become shallower and more uniform. Longer swelling time induces the formation of network of invaginated folds (Fig. 8e), then increasing compressive stress actuates occurrence of slight in-plane expansion because of sunken valley in the surface. The release of compressive stress is easier to arise in the invaginated fold as a stress defect. Thus, there is a migration of PS-PDMS molecules from network center to fold in which PS-PDMS molecules start to accumulate. By prolonging swelling time, this accumulation becomes more serious to induce local delamination and then two fold edges mainly grow normally and slightly grow parallel to surface. The valley in fold peak will not disappear until enough high compressive stress is applied to make the two edges coalesce together. Finally, the network of sharp folds can be constructed after the film undergoes transition from invaginated fold to sharp fold (Fig. 8f). Once generated successfully, the network of sharp folds tends to become denser and more complete before the stable and ordered network with a constant characteristic period is eventually constructed as the swelling time increases.

4. Conclusions

During solvent vapor swelling, for the cross-linked PS-PDMS film constrained on rigid substrate, a unique network of folds could be constructed successfully to release increasing in-plane compressive stress. We demonstrate that the wrinkled state is not essential to construct the network of folds. In this article, the slow kinetics induced by the solvent vapor swelling contributes to clearly understand the evolution process. We conclude that this network of folds is closely relative to rearrangement of PS-PDMS molecules. The balance between cross-linking constraint and impulse derived from mesostructural organization prompts formation of small holes during initial swelling stage. In fact, these small holes act as nuclei and induce the formation of invaginated folds to release compressive stress accumulated in hole rim. Thereafter, invaginated folds continuously grow into the network of invaginated folds, and then transition from invaginated fold to sharp fold will be produced to construct complete network of sharp folds accompanying with a molecule migration. At the same time, the cross-linking and network of folds have a strong influence on self-assembly behavior. For cross-linked PS-PDMS film, poorly ordered nanostructures can be fabricated while most of vertically oriented cylinders can be produced. The unique network morphology and kinetics are strongly dependent of solvent solubility parameter and saturated vapor pressure. Only when solvent solubility parameter is approximately to that of PS chains can this surface morphology be constructed successfully. By mixing two-component solvent vapors (a relatively good solvent vapor and a poor solvent vapor), the decreased partial vapor pressure reduces kinetic rate of formation of network of folds. In our system, precisely controlling condition of solvent vapor is beneficial to precisely control surface morphology. However, it is also a challenge to fabricate well-ordered morphologies of surface patterns in the absence of external factors. We believe that the formation of ordered network of folds will offer new insight for theoretical study of mechanical instability of cross-linked BCP film and broaden potential application such as micro-fluidic devices and microfabrication.

Acknowledgements

The authors acknowledge financial support from the National Natural Science Foundation of China (51173112, 51121001 and 21274095) and the Foundation of China Academy of Engineering Physics (2013B0302058). We thank Woon-Ming Lau (Chengdu Green Energy and Green Manufacturing Technology R&D Center, Chengdu, China) for carrying out the HHIC treatments.

Notes

College of Polymer Science and Engineering, State Key Laboratory of Polymer Materials Engineering, Sichuan University, Chengdu 610065, China.
*Fax: 086-28-85460690. E-mail: fengchen@scu.edu.cn (F.C.); Fax: 086-28-85461795 qiangfu@scu.edu.cn (Q.F.).
Electronic Supplementary Information (ESI) available: AFM height images of cross-linked PS and PDMS film during THF vapor swelling and cross-linked PS-PDMS film during ethanol vapor swelling. Surface morphology of annealed PS-PDMS film after RIE.

References

1 N. Bowden, S. Brittain, A. G. Evans, J. W. Hutchinson and G. M. Whitesides, *Nature*, 1998, **393**, 146-149.
2 J. A. Rogers, T. Someya and Y. Huang, *Science*, 2010, **327**, 1603-1607.
3 J. Y. Chung, A. J. Nolte and C. M. Stafford, *Adv. Mater.*, 2009, **21**, 1358-1362.
4 B. Li, Y.-P. Cao, X.-Q. Feng and H. Gao, *Soft Matter*, 2012, **8**, 5728-5745.
5 A. Dramé, T. Darmanin, S. Y. Dieng, E. Taffin de Givenchy and F. Guittard, *RSC Adv.*, 2014, **4**, 10935-10943.
6 A. C. Trindade, J. P. Canejo, L. F. V. Pinto, P. Patrício, P. Brogueira, P. I. C. Teixeira and M. H. Godinho, *Macromolecules*, 2011, **44**, 2220-2228.
7 Q. Zheng, Z. Li and J. Yang, *RSC Adv.*, 2013, **3**, 923-929.
8 M. Watanabe and K. Mizukami, *Macromolecules*, 2012, **45**, 7128-7134.
9 L. Guo, Y. Jiang, S. Chen, T. Qiu and X. Li, *Macromolecules*, 2014, **47**, 165-174.
10 M. Liu, Y. Zhang, Y. Chen, Y. Gao, T. Gao, D. Ma, Q. Ji, Y. Zhang, C. Li and Z. Liu, *ACS Nano*, 2012, **6**, 10581-10589.
11 P. Yoo and H. Lee, *Phys. Rev. Lett.* , 2003, **91**, 154502.
12 P. J. Yoo and H. H. Lee, *Macromolecules*, 2005, **38**, 2820-2831.
13 J. B. Kim, P. Kim, N. C. Pégard, S. J. Oh, C. R. Kagan, J. W. Fleischer, H. A. Stone and Y.-L. Loo, *Nat. Photonics*, 2012, **6**, 327-332.
14 L. Pocivavsek, R. Dellsy, A. Kern, S. Johnson, B. Lin, K. Y. Lee and E. Cerda, *Science*, 2008, **320**, 912-916.
15 A. Takei, L. Jin, J. W. Hutchinson and H. Fujita, *Adv. Mater.*, 2014, **26**, 4061-4067.
16 M. Guvendiren, J. A. Burdick and S. Yang, *Soft Matter*, 2010, **6**, 5795-5801.
17 J. Yoon, J. Kim and R. C. Hayward, *Soft Matter*, 2010, **6**, 5807-5816.
18 V. Trujillo, J. Kim and R. C. Hayward, *Soft Matter*, 2008, **4**, 564-569.
19 D. Breid and A. J. Crosby, *Soft Matter*, 2009, **5**, 425-431.
20 Y. Li, J. J. Peterson, S. B. Jhaveri and K. R. Carter, *Langmuir*, 2013, **29**, 4632-4639.
21 C. M. Stafford, C. Harrison, K. L. Beers, A. Karim, E. J. Amis, M. R. Vanlandingham, H.-C. Kim, W. Volksen, R. D. Miller and E. E. Simonyi, *Nat. Mater.* , 2004, **3**, 545-550.
22 K. Khare, J. Zhou and S. Yang, *Langmuir*, 2009, **25**, 12794-12799.
23 E. P. Chan and A. J. Crosby, *Adv. Mater.*, 2006, **18**, 3238-3242.
24 J. Kim, J. Yoon and R. C. Hayward, *Nat. Mater.*, 2010, **9**, 159-164.
25 K. Efimenko, M. Rackaitis, E. Manias, A. Vaziri, L. Mahadevan and J. Genzer, *Nat. Mater.*, 2005, **4**, 293-297.
26 W. H. Koo, S. M. Jeong, F. Araoka, K. Ishikawa, S. Nishimura, T. Toyooka and H. Takezoe, *Nat. Photonics*, 2010, **4**, 222-226.
27 S. Yang, K. Khare and P.-C. Lin, *Adv. Funct. Mater.*, 2010, **20**, 2550-2564.
28 A. C. Trindade, J. P. Canejo, P. Patrício, P. Brogueira, P. I. Teixeira and M. H. Godinho, *J. Mater. Chem.*, 2012, **22**, 22044-22049.
29 H. Diamant and T. A. Witten, *Phys. Rev. Lett.* , 2011, **107**, 164302.
30 S. S. Velankar, V. Lai and R. A. Vaia, *ACS Appl. Mater. Interfaces*, 2012, **4**, 24-29.
31 M. Guvendiren, S. Yang and J. A. Burdick, *Adv. Funct. Mater.*, 2009, **19**, 3038-3045.
32 T. R. Hendricks and I. Lee, *Nano Lett.*, 2007, **7**, 372-379.
33 I. Bita, J. K. Yang, Y. S. Jung, C. A. Ross, E. L. Thomas and K. K. Berggren, *Science*, 2008, **321**, 939-943.
34 Y. S. Jung, J. B. Chang, E. Verploegen, K. K. Berggren and C. A. Ross, *Nano Lett.*, 2010, **10**, 1000-1005.

35 W. Chen, J. Luo, P. Shi, C. Li, X. He, P. Hong, J. Li and C. Zhao, *RSC Adv.*, 2014, **4**, 50393-50400.

36 A. Knoll, R. Magerle and G. Krausch, *J. Chem. Phys.*, 2004, **120**, 1105.

37 S. Park, L. Tsarkova, S. Hiltl, S. Roitsch, J. Mayer and A. Böker, *Macromolecules*, 2012, **45**, 2494-2501.

38 W. van Zoelen, E. Polushkin and G. Ten Brinke, *Macromolecules*, 2008, **41**, 8807-8814.

39 A. M. Telford, S. C. Thickett, M. James and C. Neto, *Langmuir*, 2011, **27**, 14207-14217.

40 N. L. Wu, K. D. Harris and J. M. Buriak, *ACS Nano*, 2013, 7, 5595-5606.

41 Q. Wang, J. Yang, W. Yao, K. Wang, R. Du, Q. Zhang, F. Chen and Q. Fu, *Appl. Surf. Sci.*, 2010, **256**, 5843-5848.

42 C. V. Bonduelle, W. M. Lau and E. R. Gillies, *ACS Appl. Mater. Interfaces*, 2011, **3**, 1740-1748.

43 S. Karamdoust, B. Yu, C. V. Bonduelle, Y. Liu, G. Davidson, G. Stojcevic, J. Yang, W. M. Lau and E. R. Gillies, *J. Mater. Chem.*, 2012, **22**, 4881-4889.

44 D. B. Thompson, T. Trebicky, P. Crewdson, M. J. McEachran, G. Stojcevic, G. Arsenault, W. M. Lau and E. R. Gillies, *Langmuir*, 2011, **27**, 14820-14827.

45 Z. Zheng, W. M. Kwok and W. M. Lau, *Chem. Commun.*, 2006, 3122-3124.

46 J. Y. Chung, A. J. Nolte and C. M. Stafford, *Adv. Mater.*, 2009, 21, 1358-1362.

47 R. C. Hayward, B. F. Chmelka and E. J. Kramer, *Macromolecules*, 2005, **38**, 7768-7783.

48 D. Breid and A. J. Crosby, *Soft Matter*, 2011, **7**, 4490-4496.

49 A. B. Croll and A. J. Crosby, *Macromolecules*, 2012, **45**, 4001-4006.

50 P. Kim, M. Abkarian and H. A. Stone, *Nat. Mater.*, 2011, **10**, 952-957.

51 M. Belmares, M. Blanco, W. A. Goddard, 3rd, R. B. Ross, G. Caldwell, S. H. Chou, J. Pham, P. M. Olofson and C. Thomas, *J. Comput. Chem.*, 2004, **25**, 1814-1826.

Kinetic study of swelling-induced network of folds in cross-linked PS-PDMS film

Xin Xu, Xuelin Yao, Feng Chen* and Qiang Fu*

Table of contents entry: Constructing the network of folds in cross-linked PS-PDMS film through combining mesostructural organization of PS-PDMS and solvent-induced mechanical instability.